ISSN 0915-633X

NATIONAL INSTITUTE FOR FUSION SCIENCE

Estafette of Drift Resonances, Stochasticity and Control of Particle Motion in a Toroidal Magnetic Trap

Alexander.A. Shishkin

(Received - Feb. 7, 2001)

NIFS-681 Feb. 2001

RESEARCH REPORT
NIFS Series

TOKI, JAPAN

Estafette of Drift Resonances, Stochasticity and Control of Particle Motion in a Toroidal Magnetic Trap

Alexander A SHISHKIN

Institute of Plasma Physics, National Science Center "Kharkov Institute of Physics and Technology", Kharkov- 108, Ukraine,
and
Department of Physics and Technology, Kharkov "V.N. Karazin" National University, Kharkov-77, Ukraine

Abstract

A new method of particle motion control in toroidal magnetic traps with rotational transform using the *estafette* of drift resonances and stochasticity of particle trajectories is proposed. The use of the word "estafette" here means that the particle passes through a set of resonances in consecutive order from one to another during its motion The overlapping of adjacent resonances can be moved radially from the center to the edge of the plasma by switching on the corresponding perturbations in accordance with a particular rule in time In this way particles (e g cold alpha-particle) can be removed from the center of the confinement volume to the plasma periphery. For the analytical treatment of the stochastic behaviour of particle motion the stochastic diffusion coefficients $D_{\iota\iota}, D_{\iota\vartheta}, D_{\vartheta\vartheta}$ are introduced. The new approach is demonstrated by numerical computations of the test helium particle trajectories in the toroidal trap Large Helical Device.

Key words: drift resonance, drift islands, stochasticity, control of high energy particles

1. Introduction

Different tasks in fusion need the control of particle motion Among them are the removal of the "cold" alpha particles (helium ash) from a fusion reactor and in simulation experiment in modern devices, the conversion of trapped particles into passing ones to reduce the neoclassical transport , the screening of the bulk plasma from impurity ions and others. There exist different approaches to control the particle motion and one of them is to apply magnetic field perturbations to produce resonance trajectories - drift islands, overlapping of the islands and stochastic trajectories that lead, for example, to the removal of test particles from the center of the magnetic configuration to the periphery [1,2]. The drift island motion – without an overlapping of resonances is possible [3 -5].

In this paper a new approach is considered, namely the *estafette* of resonances for the particle. Here the word *estafette* (relay race) is used to describe that the particle passes through a set of resonances consistently from one to another during its motiom A new method of particle motion control in toroidal magnetic traps with rotational transform using the *estafette* of drift resonances and stochasticity of particle trajectories can be described in the following. If there are some adjacent rational drift surfaces with the drift rotational transform $\iota^* = n/m, \iota^* = n'/m'$, $\iota^* = n''/m''$, then the magnetic perturbations with the wave numbers (m,n), (m',n'), (m'',n'') can lead to some families of drift islands Overlapping of the adjacent resonance structure is the reason for the stochasticity [6] of the particle trajectories. If a particle trajectory passes through the set of perturbations this test particle can escape from the center of the confinement volume to the periphery.

Overlapping of the adjacent resonances in the local space within the plasma can be transferred outward in the process of particle motion by switching on the corresponding perturbations in accordance with a special rule in time. In such a way the particle (cold alpha-particle, for example) can be removed from the center of the confinement volume into the periphery of the plasma and the "reverse" task - the transport of the particles injected from outside the plasma into the center of the confinement volume – can be solved.

The mathematical basis of the description is rather similar to the description of the nonlinear oscillator (pendulum) with a quasi-periodic perturbation. In the theory of the nonlinear oscillator it is possible to describe the resonance phenomena, the single isolated resonance (Krylov-Bogolyubov-Mitropol'skiy method [7]) and it is stated that the chaotic states exist in the weakly nonlinear limit. For the description of the stochastic trajectory properties the diffusion coefficients $D_{\alpha.\alpha}$, $D_{\alpha.\beta}$ and $D_{\beta,\beta}$ are used, where α and β are the amplitude and phase - slowly changing variables used in the averaged method of the nonlinear theory, Kolmogorov–Arnold-Moser -Mitropol'skiy methods are developed [8].

In this paper, *estafette* of resonances is studied with both analytical methods and numerical integration of guiding center equations. The consideration is carried out in the real geometry - with the use of the coordinates r,ϑ,φ, connected with the circular axis of the torus. Stochastic diffusion coefficients $D_{r,r}, D_{r,\vartheta}, D_{\vartheta,\vartheta}$ are introduced. These coefficients are useful to evaluate the deviation of the trajectories in the radial (r) and the poloidal angular (ϑ) directions after a large number of rotations (rounds) along the torus, i.e. in the toroidal angular (φ) direction.

They are helpful to evaluate, for example, the time τ_{rr} ($\tau_{\vartheta\vartheta}$) necessary for the deviation of the particle trajectory from the initial surface in the radial (poloidal angular) direction, the time $\tau_{r\vartheta}$ necessary for the deviation of the particle trajectory from the initial surface in a certain angular space under the given deviation in the radial direction. This approach can be used in a divertor flux description and for the optimization of the divertor configuration. Stochastic diffusion coefficients for magnetic field lines were introduced in [9,10]. The concept of braided magnetic lines is very fruitful to describe the transport of plasma across destroyed magnetic surfaces [11-14].

In this paper the new physics effect – *estafette* of drift resonances of the test particle (for instance "cold" alpha-particles) in the toroidal trap with a rotational transform of the magnetic field - here the Large Helical Device is used as an example - and the removal of test particles from the center of the magnetic configuration to the periphery is shown by the numerical integration of guiding center equations. The numerical study is supported by the analytical development

The method of the *estafette* of resonances can be applied to other practical physics tasks and may be considered as a new approach in the transition to chaotic states [15].

The paper is organized as follows. The main equations are described in Section 2: the guiding center equations are in the subsection 2.1 and the main magnetic field – in sub section 2.2 and perturbations of the magnetic field in subsection 2.3. The analytical treatment is given in Section 3, where the diffusion type equation for the drift surface function is obtained (subsection 3.1) and stochastic diffusion coefficients are introduced (subsection 3.2). *Estafette* of resonances of the test particle in a real magnetic configuration with the numerical integration of particle guiding center equations is analyzed in Section 4. Coil system for the producing the perturbations, the physics mechanisms which can effect the resonance conditions are discussed in Section 5. Main conclusions are given in Section 6.

2. Main Equations

2 1 Guiding center equations

For our consideration guiding center equations are used [16]

$$\frac{d\mathbf{r}}{dt} = V_{II}\frac{\mathbf{B}}{B} + \frac{c}{B^2}[\mathbf{E}\times\mathbf{B}] + \\ + \frac{M_j c(2V_{II}^2 + V_{\perp}^2)}{2eB^3}[\mathbf{B}\times\nabla B],$$

$$\frac{dW}{dt} = e\mathbf{E}\frac{d\mathbf{r}}{dt} + \frac{M_j V_{\perp}^2}{2B}\frac{\partial B}{\partial t}, \qquad (2.1)$$

$$\frac{d\mu}{dt} = 0.$$

Here $\mathbf{r}$ is the radius-vector of the particle, $\mathbf{B}$ is the magnetic field, $\mathbf{E}$ is the electric field, V and V are the parallel and perpendicular velocities, M_j and e are mass and charge of the particle, W is the kinetic energy and μ is the magnetic moment of the particle ($\mu = \frac{M_j V_{\perp}^2}{2B}$).

2.2 Main magnetic field

The main magnetic field ($\mathbf{B} = \nabla\Phi$) is modeled with the use of the magnetic field potential

$$\Phi = B_0[R\varphi - \\ - \frac{R}{m}\sum_n \varepsilon_{n\,m}(r/a_h)^n \sin(n\vartheta - m\varphi) + \varepsilon_{1,0} r \sin\vartheta], \qquad (2.2)$$

where B_0 is the magnetic field at the circular axis, R and a_h are the major and minor radii of the helical winding; r, ϑ, φ are the coordinates connected with the circular axis of the torus, r is the radial variable, ϑ and φ are the angular variables along the minor and major circumference of the torus, ϑ increases in the direction opposite to the main normal of the circular axis of the torus, metric coefficients are the following $h_r = 1$, $h_\vartheta = r$, $h_\varphi = R + r\cos\vartheta$, m is the number of the magnetic field periods along the torus, l is the helical winding pole number The index n assumes the values $n = l,\ l-1,\ l+1$, $\varepsilon_{n\,m}$ are the coefficients of the harmonics of the magnetic field For the results presented here the parameters of the Large Helical Device [17] are taken $l = 2$, $m = 10$, $B_0 = 3$ T, $R = 390$ cm, $a_h = 97\ 5$ cm; the values of $\varepsilon_{n\,m}$ are taken in such a way that the magnetic surfaces, the magnetic field modulation along the force line and other properties coincide with the results of Ref [18] For the configuration with the inward shift of the magnetic axis the parameters are $\varepsilon_{2\,10} = 0\ 79$, $\varepsilon_{3\,10} = -0.032$, $\varepsilon_{1\,10} = -0.056$, $\varepsilon_{1\,0} = 0.045$

2 3 The perturbation magnetic field

The perturbation magnetic field considered here is given with the scalar potential

$$\Phi_p = B_0 a_h \frac{\varepsilon_{m\,n.p}}{m_p}\left(\frac{r}{a_h}\right)^{m_p}\sin(m_p\vartheta - n_p\varphi + \delta_{m.n\,p}) \qquad (2.3)$$

The "wave numbers", amplitude and phase values of the perturbing magnetic field should be chosen in accordance with the rational values of the drift rotational transform of the resonant particle In the case considered below these parameters are the following: m_p=4, n_p=3; $\varepsilon_{4\,3.p}$= 0.003, $\delta_{4\,3.p} = \pi/2$; m_p= 5, n_p=4 $\varepsilon_{5\,4\,p}$=0.007, $\delta_{5.4.p} = 0$; m_p= 10, n_p=9 $\varepsilon_{9\,10\,p}$=0 03, $\delta_{9\,10\,p} = 0$; all explanations can be found in Section 4.2.

3. Analytical Treatment

3.1 Equation for the Drift Flux Surface Function

As is known [19,20], particle motion can be described with the integrals of the equation system (2 1) and one of them is the function of the drift surface $\Psi^*(r,\vartheta,\varphi,V_{\parallel},V_{\perp},t)$ We assume that the flux of particle guiding centers is conserved during the particle motion in analogy with the magnetic flux. This leads to

$$\Psi^*(r,\vartheta,\varphi,V_{\parallel},V_{\perp},t)=const \quad (3.1)$$

and the total derivative of the drift surface function is equal to zero

$$\frac{d\Psi^*}{dt}=0. \quad (3.2)$$

The equation (3.2) in variables r,ϑ,φ and $V_{\parallel}$, $V_{\perp}$ takes the form

$$\frac{\partial\Psi^*}{\partial t}+\frac{dr}{dt}\frac{\partial\Psi^*}{\partial r}+\frac{rd\vartheta}{dt}\frac{\partial\Psi^*}{r\partial\vartheta}+\frac{Rd\varphi}{dt}\frac{\partial\Psi^*}{R\partial\varphi}+$$
$$+\frac{dV_{\parallel}}{dt}\frac{\partial\Psi^*}{\partial V_{\parallel}}+\frac{dV_{\perp}}{dt}\frac{\partial\Psi^*}{\partial V_{\perp}}=0. \quad (3.3)$$

After substituting the equations for $\frac{dr}{dt},\frac{rd\vartheta}{dt},\frac{Rd\varphi}{dt}$ and $\frac{dV_{\parallel}}{dt},\frac{dV_{\perp}}{dt}$ from equation system (2.1) into (3.3) we obtain

$$\frac{\partial\Psi^*}{\partial t}+\frac{V_{\parallel}}{B}\left(\mathbf{B}\nabla\Psi^*\right)+$$
$$\frac{Mc}{2eB^3}\left(2V_{\parallel}^2+V_{\perp}^2\right)\left([\mathbf{B}\times\nabla B]\nabla\Psi^*\right)- \quad (3.4)$$
$$\frac{V_{\perp}^2}{B^2}(\mathbf{B}\nabla B)\frac{\partial\Psi^*}{\partial V_{\parallel}}+\frac{V_{\parallel}}{4B^2}(\mathbf{B}\nabla B)\frac{\partial\Psi^*}{\partial V_{\perp}^2}=0$$

In our following consideration we assume that $\frac{\partial\Psi^*}{\partial V_{\parallel}}=0$ and $\frac{\partial\Psi^*}{\partial V_{\perp}^2}=0$. These derivatives are very important when the transition of a particle from a trapped one into a passing one is studied. However they are not so important for the study of the resonant passing particle in the narrow range of $V_{\parallel}$ and $V_{\perp}$ especially, when the spreading of $\Psi^*=const$ contours due to magnetic field perturbations is considered

We take here the simplified form of the magnetic field with the rotational transform $\iota(r^2)$

$$\mathbf{B}_0=B_0\left\{0,\frac{r}{R}\iota(r^2),\frac{1}{1+(r/R)\cos\vartheta}\right\} \quad (3.5)$$

and for the perturbations

$$\mathbf{B}_{m,n}=B_0\begin{Bmatrix}b_{m,n}(r/a)^{m-1}\sin(m\vartheta-n\varphi+\delta_{m,n}),\\ b_{m,n}(r/a)^{m-1}\cos(m\vartheta-n\varphi+\delta_{m,n}),\\ 0\end{Bmatrix} \quad (3.6)$$

and

$$\widetilde{\mathbf{B}}=B_0\begin{Bmatrix}b_{m',n'}(r/a)^{m'-1}\sin(m'\vartheta-n'\varphi+\delta_{m',n'}),\\ b_{m',n'}(r/a)^{m'-1}\cos(m'\vartheta-n'\varphi+\delta_{m',n'}),\\ 0\end{Bmatrix} \quad (3.7)$$

Then the equation for $\Psi^*_{0,m,n}$ can be reduced to the following form

$$\frac{\partial\Psi^*_{0,m,n}}{\partial t}+\frac{V_{\parallel}}{B}\left(\mathbf{B}_{0,m,n}+\widetilde{\mathbf{B}}\right)\nabla\Psi^*_{0,m,n}+$$
$$+\frac{Mc}{2eB^3}\left(2V_{\parallel}^2+V_{\perp}^2\right)\left[\left(\mathbf{B}_{0,m,n}+\widetilde{\mathbf{B}}\right)\times\nabla B\right]\nabla\Psi^*_{0,m,n}=0, \quad (3.8)$$

where

$$\mathbf{B}_{0,m,n}=\mathbf{B}_0+\mathbf{B}_{m,n} \quad (3.9)$$

We suppose that under the magnetic field $\mathbf{B}_{0,m,n}$ the function $\Psi^*_{0,m,n}$ is satisfied with the equation

$$\frac{V_{\parallel}}{B}\left(\mathbf{B}_{0,m,n}\nabla\Psi^*_{0,m,n}\right)+$$
$$+\frac{Mc}{eB^3}\left(2V_{\parallel}^2+V_{\perp}^2\right)\left[\mathbf{B}_{0,m,n}\times\nabla B\right]\nabla\Psi^*_{0,m,n}=0. \quad (3.10)$$

The function $\Psi^*_{0,m,n}$ is described with the expression [4]

$$\Psi^*_{0,m,n}=\int\left[m\iota(r/a)^2-n\right]dr+$$
$$+Rb_{m,n}\left(\frac{r}{a}\right)^{m-1}r\cos(m\vartheta-n\varphi+\delta_{m,n})-$$
$$-\frac{McV_{\parallel}}{eB_0}\left(1+\frac{V_{\perp}^2}{V_{\parallel}^2}\right)\frac{m\iota(r/a)^2-n}{\iota(r/a)^2}r\cos\vartheta. \quad (3.11)$$

Then under the effect of $\tilde{\mathbf{B}}$ we find the change of Ψ^*_{0mn} in the following way

$$\Psi^*_{0mn}\Big|_{\mathbf{B}} = \Psi^*_{0mn}\Big|_{\mathbf{B}_0} + + \Delta r\frac{\partial\Psi^*_{0mn}}{\partial r} + r\Delta\vartheta\frac{\partial\Psi^*_{0mn}}{r\partial\vartheta}, \tag{3.12}$$

Δr and $r\Delta\vartheta$ are due to $\tilde{\mathbf{B}}$

Then the equation (3.8) reduces to the following one

$$\frac{\partial\Psi^*_{0mn}}{\partial t} + \left(\tilde{V}_r + \tilde{V}_r\frac{\partial}{\partial r}\Delta r + \tilde{V}_\vartheta\frac{\partial}{r\partial\vartheta}\Delta r\right)\frac{\partial\Psi^*_{0mn}}{\partial r} +$$

$$+\left(\tilde{V}_\vartheta + \tilde{V}_r\frac{\partial(r\Delta\vartheta)}{\partial r} + \tilde{V}_\vartheta\frac{1}{r}\frac{\partial(r\Delta\vartheta)}{\partial\vartheta} - \tilde{V}_r\frac{\Delta\vartheta}{r}\right)\frac{\partial\Psi^*_{0mn}}{r\partial\vartheta}$$

$$+D_{rr}\frac{\partial^2\Psi^*_{0mn}}{\partial r^2} + D_{r\vartheta}\frac{\partial^2\Psi^*_{0mn}}{r\partial r\partial\vartheta} + D_{\vartheta\vartheta}\frac{\partial^2\Psi^*_{0mn}}{r^2\partial\vartheta^2} = 0 \tag{3.13}$$

Here such designations are introduced

$$\tilde{\mathbf{V}} \equiv \frac{V}{B}\tilde{\mathbf{B}} + \frac{Mc}{2eB^3}\left(2V^2 + V_\perp^2\right)\left[\tilde{\mathbf{B}}\times\nabla B\right] \tag{3.14}$$

and

$$D_{rr} \equiv \tilde{V}_r\Delta r, \quad D_{r\vartheta} \equiv \tilde{V}_r r\Delta\vartheta + \tilde{V}_\vartheta\Delta r, \quad D_{\vartheta\vartheta} \equiv \tilde{V}_\vartheta r\Delta\vartheta \tag{3.15}$$

3.2. Stochastic Diffusion Coefficients

Stochastic diffusion coefficients can be evaluated using

$$D_{rr} = \tilde{V}_r\Delta r \cong \left(\frac{V}{B}\right)^2(B_{mn,r}\tilde{B}_r + \tilde{B}_r^2)\frac{2\pi R}{V},$$

$$D_{r\vartheta} = \tilde{V}_r r\Delta\vartheta + \tilde{V}_\vartheta\Delta r \cong$$

$$\cong 2\left(\frac{V}{B}\right)^2(B_{mn,r} + \tilde{B}_r)(B_{mn\vartheta} + \tilde{B}_\vartheta)\frac{2\pi R}{V}$$

$$D_{\vartheta\vartheta} = \tilde{V}_\vartheta r\Delta\vartheta \cong \left(\frac{V}{B}\right)^2(B_{mn\vartheta}\tilde{B}_\vartheta + \tilde{B}_\vartheta^2)\frac{2\pi R}{V} \tag{3.16}$$

It should be noted that the sense of the diffusion coefficients is the following

$$D_{rr} = \frac{(\delta r)^2}{\tau_{rr}}, \quad D_{r\vartheta} = \frac{r\delta r\delta\vartheta}{\tau_{r\vartheta}}, \quad D_{\vartheta\vartheta} = \frac{r^2(\delta\vartheta)^2}{\tau_{\vartheta\vartheta}}. \tag{3.17}$$

From the expressions (3.17) (after substituting from (3.16)) we can evaluate, for example, the time τ_{rr} necessary for the deviation of particle trajectories from the initial surface in the radial direction, the time $\tau_{r\vartheta}$ necessary for the deviation of particle trajectories from the initial surface in a certain angular space under a given deviation in the radial direction and the time $\tau_{\vartheta\vartheta}$ for the deviation of the particle trajectories in the angular direction

The stochastic diffusion coefficients obtained are the local characteristics and depend on the variables r, ϑ We should remember that these diffusion coefficients describe the breaking of the separatrix that separates the m/n islands on the drift surface with the drift rotational transform $\iota^* = n/m$ from the adjacent resonance m'/n' islands on the drift surface with $\iota^* = n'/m'$ If we put the expressions for the magnetic field components (3.6) and (3.7) in (3.16) we can see that the stochastic diffusion coefficients depend on the variables r, ϑ.

One possible question can arise, namely, at which condition the drift islands can overlap and when the coefficients $D_{rr}, D_{r\vartheta}, D_{\vartheta\vartheta}$ can be used.

As it is known the maximum transverse size of the drift island can be described by the following expression [4]

$$\Delta r_{n,m} = \left(\frac{2Rab_{n,m}(r_{n,m}/a)^m}{m(d\iota/dr^2)\big|_{r=r_{n,m}}}\right)^{1/2} \tag{3.18}$$

where $r_{n,m}$ is the radius of the magnetic surface with $\iota(r_{n,m}) = n/m$ and when the adjacent islands can overlap i.e when [6]

$$K \equiv \frac{\Delta r_{n,m} + \Delta r_{n',m'}}{r_{n',m'} - r_{n,m}} \geq 1,\ (r_{n',m'} - r_{n,m} > 0) \quad (3.19)$$

then the stochasticity of the particle trajectory can occur.

Analytical expressions obtained in this paper can be used for the optimization of the magnetic field perturbations (the sets of "wave" numbers, amplitudes, phases) which can lead to stochastization of the test particle trajectories and the preservation of the drift surfaces of the bulk plasma particles. Obtaining such conditions is the subject of future work.

Here it is shown that under the perturbations with the "wave" numbers (m', n') the separartrix of the (m,n) resonance is broken and the particle trajectories become stochastic Thus the particle can wander from one resonance (initial) to another resonance – adjacent to the initial one and then this phenomenon repeats, the particle passes step by step through the set of resonances and can escape from the center of the confinement volume to the periphery and vice versa from the periphery into the center of the confinement volume. In such a way the impurity ions (cold alpha-particles, for instance) can be removed from the magnetic trap. In the same way, the transport of high energy particles from the periphery of the confinement volume into the center can be realized.

4. Estafette of Resonance and Helium Ion Removal

In order to perform further investigation and to demonstrate the main physics effects, the numerical integration of the guiding center equation system (2.1) with the use of the main magnetic field in the form (2.2) and the magnetic perturbation field (2.3) is carried out. A fourth order Runge-Kutta method is used for the numerical integration of the guiding center equations.

For analysis here the configuration for the Large Helical Device (LHD) – the most advanced steady-state helical device which is under successful operation at the National Institute for Fusion Science (Toki, Japan) – is chosen The possibility of the experimental study of cold alpha-particles on LHD (simulation experiment) has already been discussed [21].

4.1 Test Particle

Helium ions ($_2He^4$) with the energy W=100 keV and starting pitch V_{II}/V = 0.9 are taken as the test particles Starting point coordinates are r_0=3, 7, 11, 15, 19 cm, at ϑ_0=0 and φ_0=0. Here r_0, ϑ_0 and φ_0 are the coordinates of the starting (launching) points of the particles. The starting points in the Figures below are designated with the large crosses. It should be noted that there is a difference between the radial coordinates of the launching points (which are referenced from the circular axis of the torus) and the averaged radii of the drift surfaces because the drift surface axis shifts relative to the position of the circular axis of the torus.

4.2. Drift Surfaces without Perturbations

The so-called Inward Shift configuration is taken where the magnetic axis is shifted toward the torus center and the rotational transform varies from $\iota(0) \approx 0.6$ till $\iota(a_p) \approx 1.0$. Thus rational values of $\iota(r^2/a^2)$ such as 0.75, 0.8, 0.9,1.0 can be used. Among the rational values of the drift rotational transform angle the following set is chosen $\iota(r^2/a^2) \approx$ 0.75, 0.8, 0.9,1.0 (Fig.1) and the corresponding magnetic field perturbations can be introduced. Below in subsection 5.1, where the coil system for producing the perturbations is discussed, there is an explanation for why namely these resonances are used here.

4.3 Drift Surfaces with Perturbations

4.3.1 Splitting of Resonant Surfaces

All perturbations act (switched on) simultaneously

Under the set of perturbations m_p=4, n_p=3; $\varepsilon_{4\,3\,p}$= 0.003, $\delta_{4\,3\,p} = \pi/2$, m_p= 5, n_p=4 $\varepsilon_{5\,4,p}$=0.007, $\delta_{5\,4\,p} = \pi/2$, m_p=9, n_p=10; $\varepsilon_{9\,10\,p}$= 0.03, $\delta_{9\,10\,p} = 0$; m_p= 5, n_p=5, $\varepsilon_{5\,5\,p}$=0.00, $\delta_{5\,5\,p} = 0$, - some families of drift islands in the vertical cross-section (meridional cross-section of torus) appear (Fig 2). For the drift surfaces with the drift rotational transform angle ι^*=3/4 four drift islands take place, for ι^*=4/5 five drift islands appear, the surface with ι^*=9/10 does not split but is corrugated and one island appears instead at the drift surface with ι^*=1/1 It should be noted that the amplitude of the perturbation with m_p=5, n_p=5 is equal to zero The one island at ι^*=1/1 is the result of the interaction of all magnetic field harmonics.

4.3.2 Stochasticity of Drift Trajectories

Perturbations switched on in the strict sequence

This is the most interesting effect. The perturbations are switched on in a strict sequence as is shown in Fig 3a. The amplitudes of the perturbations with m_p= 5, n_p=4 and m_p=9, n_p=10 are 1.4 times larger than in Fig 2 Another very important fact is that the perturbation with $m_p/n_p = 5/4$ is switched on at the moment of time when the radial deviation of the test particle is the largest Therefore the test particle starting at the point with $r_0 = 7$ cm, $\vartheta_0 = 0.0$, $\varphi_0 = 0.0$ can move from the initial magnetic surface to the following magnetic surfaces, i.e. from the center of the confinement volume to the periphery. This is seen in Figure 3b. The radial variable of the particle trajectory increases in time and achieves a value at the periphery (marked by a "cross") of the confinement volume (Fig 3c) where it may be removed by mechanical means It is possible to mark out the interval of time when the particle is in resonance with the $m_p/n_p = 4/3$ perturbation, then the interval of time when the particle is in resonance with the $m_p/n_p = 5/4$ perturbation and finally the time when it leaves the plasma Stochasticity of the trajectories with different but rather close starting points and their reciprocal penetration is shown on Fig.4a. The dependence of the radial variable on the angular variable (Fig 4b) demonstrates the diffusive character of the trajectory. We would like to emphasize that in Fig 3c and Fig 4b the footprints of the full trajectory are gathered together while in Fig. 4a (and Fig. 1, 2b, 3b) only the footprints from the "same name" vertical cross-sections are taken into account. To observe the stochastization of the particle trajectory is more convenient to use the vertical cross-sections of the drift surfaces while to evaluate the maximum deviation of the radial variable and the deviation of the angular variable of the particle it is necessary to use the full particle trajectory

We have considered here two cases.

In the first case the perturbations are switched on simultaneously but they have the small amplitudes and do not lead to stochastization of the trajectory. The drift islands are present but they are not overlapped. The deviation of the particle from the initial surface is the island width size

In the second case the perturbations with the larger amplitudes are switched on consequetively in time The test particle escapes from the confinement volume following the resonances consequetively, one after another as is expected in accordance with the *estafette* of resonances. The second case is preferable because the "cold" alpha-particle escapes and the drift surfaces of the bulk plasma ions and electrons are not destroyed If these perturbations (with larger amplitudes) are switched on at the same moment of time (all of them from the beginning) the particle escapes from the confinement volume earlier but destruction of drift surfaces of other particles, particularly bulk plasma ions takes place.

One practical question is how the switching times of perturbation modes are chosen. Here we follow the particle trajectories and fix the time when the trajectory deviation in the radial direction (variable r) achieves the maximum value under the resonance $\iota^* = n_p / m_p$. Then the perturbation with the following set of "wave" numbers (n'_p, m'_p) satisfying the resonance condition $\iota^* = n'_p / m'_p$ is switched on and this process should continue.

4.3.3. Selectivity of Stochastic Transport

One important question is why the bulk plasma ions and electrons do not escape while the helium ion leaves the confinements volume First of all below we describe the examples of the trajectories of the bulk plasma ion and electrons starting at the same launching point (initial point) as the helium ion. Then we summarize the computation results for all launching points taken here (Fig.5)

Bulk plasma ions motion

If a deuterium ion with energy $W = 7$ keV (the possible thermal energy of the bulk ion plasma in the device considered) starts at the point where its trajectory drift rotational transform ι^*=4/5 then this particle forms 5 islands in the vertical cross-section instead of 4 islands as in the case of the helium ion with $W =$ 100 keV. The trajectory of the particle with energy $W = 7$ keV is not stochastic, the islands are not destroyed.

Bulk plasma electron motion

Electrons with the energy $W = 7$ keV starting at the same point have the drift rotational transform ι^*=0.836 (computational value). Their drift surface have some corrugation but are not stochastic.

The computational drift angle of the bulk plasma electron and ion is different from the computational drift angle of helium ion (Fig.5). That is why the bulk particles are not involved in the process of *estafette* of resonances and do not escape from the confinement volume.

4.3.4 Fraction of Helium Particles Involved in Stochastic Transport (Statistics)

Helium ions with energy $W = 100$ keV, starting pitch $V_{II} / V =$ 0.9 and with starting points as shown in Fig 6 (open circles) come to the periphery of the confinement volume (closed circles). These points are chosen in such a way that they gather in the upper part of the confinement volume. These particles can be collected and removed by mechanical means. The footprints of particles are shown on the background of the drift surfaces from Fig.2b. The time for escape of the test particles is approximately the same and is equal to 1×10^{-3} s.

5. Discussion

5.1. Coil system for producing the perturbations

There exist some practical ways to produce the perturbations and create the conditions for diverting the plasma with the use of stochasticity , for example [22-29]. For the purpose of the *estafette* of resonances a system like the one described in [22-24] can be used. The number of coils N should be proportional to the product of m_p for the set of perturbing harmonics, more exactly to the least common multiple of the numbers in the denominator of the rational values. Here a set of perturbations is used which corresponds to the following rational values:3/4, 4/5, 9/10,1/1 Of course, there exist other resonances, such as 2/3, 5/6, 6/7, 7/8, 8/9 etc. However only several main resonances, namely 3/4, 4/5, 9/10 1/1 are used in this study. The reason is that the product of the numbers which are in the denominator of the rational values should determine the number of the current ring coils which can produce the magnetic field perturbations with the corresponding set of "wave" numbers. It is desirable that the number of the coils, N, would be not too large.

It is possible to use a more internal resonance such as drift surface with $\iota^* = 2/3$ and magnetic perturbation with $m_p / n_p = 3/2$ In this case the family of 3 islands appear in the meridional cross-section. The dimensions of other islands and resonant surfaces changes too

5 2 Effect of other physics mechanisms

The electric field does not affect the resonance condition for high energy particle ("cold" alpha-particles) strongly Stochasticity takes place if an electric field with $e\Phi / W = \pm 0$ 1 is present

The effect of scattering on the resonance studied in [30, 31] has shown that there exist the conditions when the resonances are not broken

5 3. Other possibilities to use the described mechanism

The physical mechanism described here can be applied to solve the "reverse" task- the transport of particles injected from outside the plasma into the center of the confinement volume In such a way it is possible to inject fueling particles if it is necessary

5 4. About the onset of the chaotic motion in deterministic Hamiltonian systems

As it is known (see for example [9, 10, 15. 33-35]) the chaotic motion can be the property of many dimensional dynamic systems (with many degrees of freedom) and "low number"-dimensional dynamics system (with a small number degrees of freedom) also. The trajectory of the particle motion belongs to "low number "dimensional systems Such a system also can experience stochastization

This is a very important issue. The particle trajectory is described by the equation of the non linear oscillator. In the case of the *estafette* of resonances guiding center equations can be reduced to the non linear oscillator under quasi periodic perturbation. Analysis of the oscillator equation in phase space is a commonly known tool of study However practical tasks and many applications need the analysis in real geometry space Overlapping of resonances of particle trajectories can lead to stochasticity in the real space It can be seen on stellarators. That is why the description of these effects should be done in real space coordinates. Such analytical description is given in this paper in section 3 and numerical demonstration is presented in Section 4

5.5 Possible scenario of the *estafette* resonances application

Here we assume that the helium ions with a certain energy and the parallel velocity are at a certain location in the center of the confinement volume and we demonstrate one way to remove them from the center of the confinement volume to the outside with no deterioration of the plasma ion confinement. Another possible scenario can be the following: if the ions which should be removed are observed at a certain place and their energy and parallel velocity are determined then their drift rotational transform angle should be calculated, the set of mode numbers of the externally applied magnetic field perturbations are chosen and after the switching on the corresponding perturbations the particles can be removed.

6. Conclusions

The principal possibility of the new physics mechanism - *estafette* of resonances is shown here

1 *Estafette* of drift resonances can be used for the removal of a test particle, particularly helium ash, when the perturbing magnetic fields are externally applied For this purpose in the case of particle trajectories with the drift rotational transform $\iota^* = n_p / m_p$ the perturbing magnetic field with wave numbers m_p, n_p leads to drift island formation. If the adjacent drift islands overlap the particle trajectories become stochastic A particle

passes through a set of adjacent resonances and can leave the confinement volume.

2. This mechanism to remove the ash from the confinement volume or to control the particle motion inside the confinement volume is selective relative to the energy. The bulk plasma ions do not experience the stochastisation of their trajectories and do not escape the plasma.

3. The efficiency of this approach is evaluated (partly) from the statistics. For each case a concrete scenario as described above and applied to this mechanism should be developed

4. Perturbing magnetic fields can be produced by a system of coils with specific currents. The system of coils is not so complicated and can be similar to the coils of the local island divertor. The effectiveness of the method proposed here will be studied in a future work.

Acknowledgments

The author expresses his deep gratitude to Prof. Tom Dolan (IAEA) for his continuous support and thanks Dr. B. Peterson and Mr. M.Yakovlev for their help in improving this article. The author is very grateful to Prof. K.Yamazaki, Prof. O.Motojima and General Director Prof. M.Fujiwara for the invitation to come to the National Institute for Fusion Science and Prof. Ch.Namba for his support.

References

[1]. Mynick, H.E. *Transport of energetic ions by low- n magnetic perturbations.* Phys Fluids B **5** (1993) 2461.

[2] Mynick, H.E. *Stochastic transport of MeV ions by low- n magnetic perturbations.* Phys.Fluids B **5** (1993) 1471.

[3]. Mynick, H.E., Pomphrey, N. *Frequency Sweeping: A New Technique for Energy-Selective Transport* ,Nuclear Fusion **34** (1994) 1277.

[4]. Motojima, O., Shishkin, A.A. *Drift Island Motion in Helical Plasma and its Use for Ash Removal and High Energy Ion Injection,* Plasma Physics and Controlled Fusion **41** (1999) 227.

[5]. Shishkin A.A., Zolotukhin A.V. *Drift Resonance of Impurity Ions in a Toroidal Magnetic Trap with Rotational Transform,* Physics of Plasmas **7** (2000) 5023

[6]. Chirikov, B.V *A universal instability of many-dimensional oscillator system.* Phys. Rep. **52** (1979) 263.

[7]. Bogolyubov, N.N. and Mitropol'skiy Yu.A. *Asymptotic Methods in the Theory of Nonlinear Oscillations,* Gordon and Breach, New York, 1962 (Russian orginal, Gos.izdat Phys.-Mat Lit, Moscow 1963)

[8]. Mitropol'skiy Yu.A. *Averaged Method in Nonlinear Mechanics,* Naukova Dumka, Kiev 1971, 440 pages (in Russian).

[9]. Rosenbluth, M.N., Sagdeev, R.Z., Taylor, J.B., Zaslavski, G.M. *Destruction of magnetic surfaces by magnetic field irregularities,* Nuclear Fusion **6** (1966) 297.

[10]. Filonenko, N. N., Sagdeev, R. Z., Zaslavski, G.M. *Destruction of magnetic surfaces by magnetic field irregularities II,* Nuclear Fusion **7** (1967) 253.

[11]. Stix T.H. *Plasma transport across a braided magnetic field.* Nuclear Fusion **18** (1978)
353.

[12]. Mendonca J.T. *Diffusion of magnetic field lines in a toroidal geometry,* Phys. Fluids B **3** (1991) 87

[13]. Hatori T., Irie, H., Abe, Y., Urata K. *Chaotic Magnetic Field Line in Toroidal Plasmas.,* Progress Theor. Phys. Suppl. 1989, No.89, p. 83 and Institute of Plasma Physics,

Research Report IPPJ-911, May 1989, Nagoya , Japan

[14] Rechester, A B . Rosenbluth, M N *Electron heat transport in a tokamak with destroyed magnetic surfaces.* Phys.Rev Lett **40** (1978) 38

[15] Grishchenko, A D , Vavriv, D M *Dynamics of a pendulum with a quasiperiodic perturbation.* Tech Phys. **42** (1997) 1115

[16] Morozov, A.I , Solov'ev, L S *Motion of Charged Particles in Elelctro-magnetic Fields,* Reviews Plasma Physics (edit by Acad M.L Leontovich) vol 1, Consultants Bureau, New York, 1996, p 201-297

[17]. Iiyoshi, A., Fujiwara, M , Motojima, O., Ohyabu, N Yamazaki, K., *Design study for the Large Helical Device.* Fusion Technology **17** (1990) 169.

[18] Shishkin, A.A , Watanabe, K N., Yamazaki, K , Motojima, O., Grekov,D.L , Smirnova, M.S , Zolotukhin, A.V., *"Some Features of Particle Orbit Behavoir in LHD Configurations"* National Institute for Fusion Science, Research Report NIFS Series, NIFS – 211, March 1993, Nagoya, Japan, 44 pages

[19]. Popryadukhin A.P. *Perturbations of the particle motion in a stellarator.* Plasma Physics, **8** (1966) 169.

[20] Solov'ev, L.S. and Shafranov, V.D. *Plasma Confinement in Closed Magnetic Sysytems (Reviews of Plasma Physics vol.5)* ed. M A.Leontovich (New York: Consultants Bureau) pp 1-247.

[21]. Sato, K N., Murakami, S., Nakajima, N., Itoh, K. *Possibility of Simulation Experiments for Fast Particles in the Large Helical Device (LHD),* Nuclear Fusion **35** (1995) 1563.

[22] Komori, A Ohyabu, N , Watanabe, T et al , Plasma Physics and Controlled Nuclear Fusion Research, 1994, Sevile, *Local island divertor concept for LHD,* Proc 15th Intern Conference, Seville,1994, IAEA, Vienna, 1995, vol 2, p 773

[23] Ohyabu, N., Komori, A , Akaishi, K et al , *Innovative divertor concepts for LHD,* Journal of Nucl Materials **220-222** (1995) 298

[24] Motojima, O , Ohyabu, N , Komori, A. et al., *Divertor experiment in large helical device,* Plasma Physics and Controlled Fusion **38** (1996) A77

[25]. Shabrov, N V , Khvesjuk, V I., Lyakhov, A N *Selective Ions Pumping from an Axisymmetric Mirror Trap,* Proc International Conference on Open Plasma Confinement Systems for Fusion, ed A.Kanantsev, Budker Institute of Nuclear Physics, Siberian Branch, Russian Academy of Sciences, 1993, World Scientific, Singapore 1994, pp 245 – 260

[26]. Shishkin, A A., Motojima, O *Coil System for the Resonant Pumping In Out of Particles in Toroidal Magnetic Traps.* 10th International Toki Conference on Plasma Physics and Controlled Nuclear Fusion (ITC-10) "Physics and Technology for Steady State Plasmas", January 18-21, 2000, Toki-city, Japan, PI-52, Abstracts, p.104 and Journal of Plasma and Fusion Research SERIES, v.3 (2000) pp.509-512

[27]. Finken, K.H , Abdullaev, S.S., Kaleck, A., Wolf G H. *Operating space of Dynamic Ergodic Divertor for TEXTOR 94,* Nuclear Fusion **39** (1999) 637.

[28] Kobayashi, M , Tuda, T., Tashiro, K. et al., *Interaction of Externally Applied Rotating Helical Field with Tokamak Plasma,* Nuclear Fusion (to be published).

[29]. Kikuchi, Yu., Tashiro, K., Kobayashi, M. et al , *Improvement of Local Helical Coil Configuration for Dynamic Ergodic Divertor*

10th International Toki Conference on Plasma Physics and Controlled Nuclear Fusion (ITC-10) "Physics and Technology for Steady State Plasmas", January 18-21, 2000, Toki-city, Japan, PI-22, Abstracts, p.74.

[30]. Sivukhin, D.V. *Coulomb Collisions in a Fully Ionized Plasma,* Reviews Plasma Physics (edit. by Acad. M.L.Leontovich) vol.4, Consultants Bureau, New York, 1996, p.93-241.

[31]. Shishkin, A.A., Motojima, O., Polunovskij, E.I. *The Motion of Drift Island in Toroidal Magnetic Trap under Coulomb Scattering,* Tech. Phys. Lett. **25** (1999) 725.

[32]. Shishkin, A.A., Sidorenko, I.N., Wobig, H *Dynamical Control of Drift Resonances in HELIAS Configuration,* 6th Ukrainian Conference and School on Plasma Physics and Controlled Fusion, Alushta, Ukraine, September 14-20, 1998, Report A -18; Problems of Atomic Science and Technology, SERIES: Plasma Physics, ISSUES 1(1), 2(2), National Sciende Center "Kharkov Institute of Physics& Technology, Kharkov, 1999.

[33]. Klafter, J., Shlesinger, M.F. and Zumofen, G. *Beyond Brownian Motion,* Physics Today **49** (2) (1996) 33.

[34]. Lichtenberg, A.J. and Liberman, A *Regular and Stochastic Motion,* Springer-Verlag, New York, 1983.

[35]. Zaslavsky, G.M *Chaos in dynamical systems,* Harwood, Chur, 1985

Figure Captions

Fig.1. Cross-sections of the drift surfaces of helium ions with the energy W=100 keV, $V_{\parallel}/V$=0.9 with the starting point coordinates r_0=3, 7.1, 11, 15.9, 19 cm, ϑ_0=0 and φ_0=0 without perturbations; time of the observation $\tau_{observ}=1.22\times10^{-3}$ s for all starting points except $r_0 = 19$ cm where $\tau_{observ}=2.44\times10^{-3}$ s.

Fig.2. Amplitudes of the perturbations (a) and cross-sections of the drift surfaces of the helium ions with the energy W=100 keV, $V_{\parallel}/V$=0.9 with the starting point coordinates r_0=3, 7, 11, 15, 19 cm, ϑ_0=0 and φ_0=0 under the set of perturbations indicated in Section 4.3.2 (b). The time of the observation is $\tau_{observ}=1.22\times10^{-3}$ s

Fig. 3. Amplitudes of perturbations in dependence on time (a), diffusion of the drift surface of the test helium ion with the starting point r_0=7 cm, (b), radial variable of the test particle trajectory in dependence on time (c); the time of observation is $\tau_{observ}=1.5\times10^{-2}$ s

Fig. 4. Diffusion of two drift surfaces for the test helium ions with the starting points r_0=7 cm (dots) and r_0=11 cm (crosses) (a), "angle versus radius" of the test helium ion trajectory (with the starting point r_0=7 cm) demonstrating the diffusion in "radius–poloidal angle" space.

Fig.5. Computational drift transform angle ι^* versus the launching point radial coordinate r_0 (ϑ_0=0, φ_0=0) for helium ion with $W = 100$ keV, V_{II}/V=0.9, electron and deuterium ion with $W = 7$ keV, V_{II}/V=0.9 and V_{II}/V=0.6

Fig.6. Statistics for the removal of helium ions with W=100 keV, V/V=0.9 . Starting points are denoted with open circles and the points of maximum distance in the Z direction are denoted with closed circles.

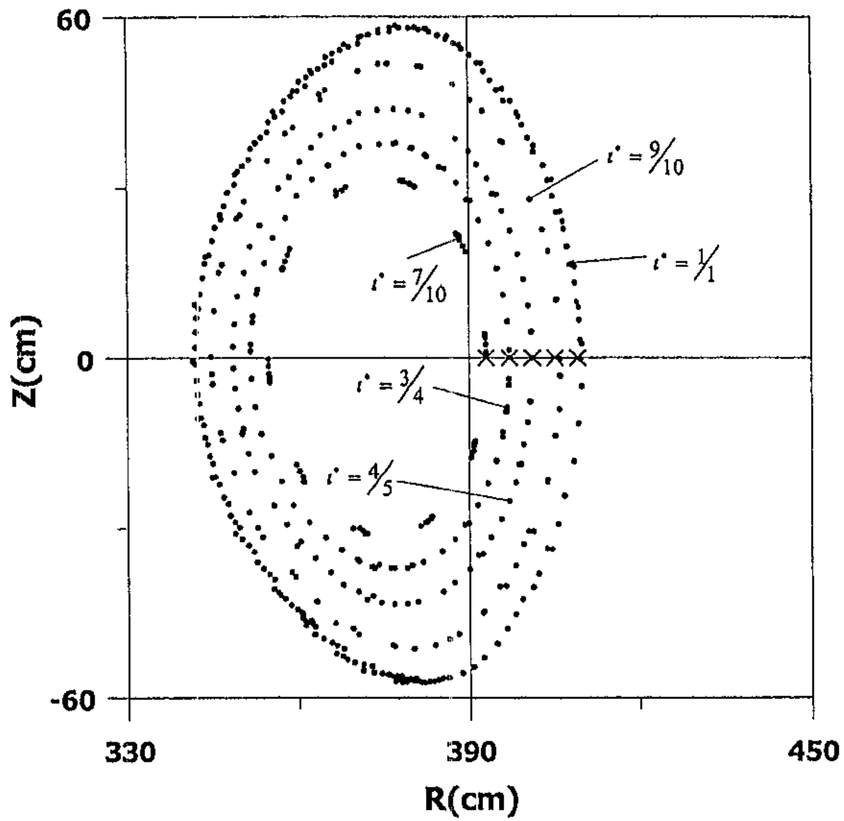
60
0
-60
Z(cm)
330
390
450
R(cm)
ι' = 9/10
ι' = 1/1
ι' = 7/10
ι' = 3/4
ι' = 4/5

Fig.1

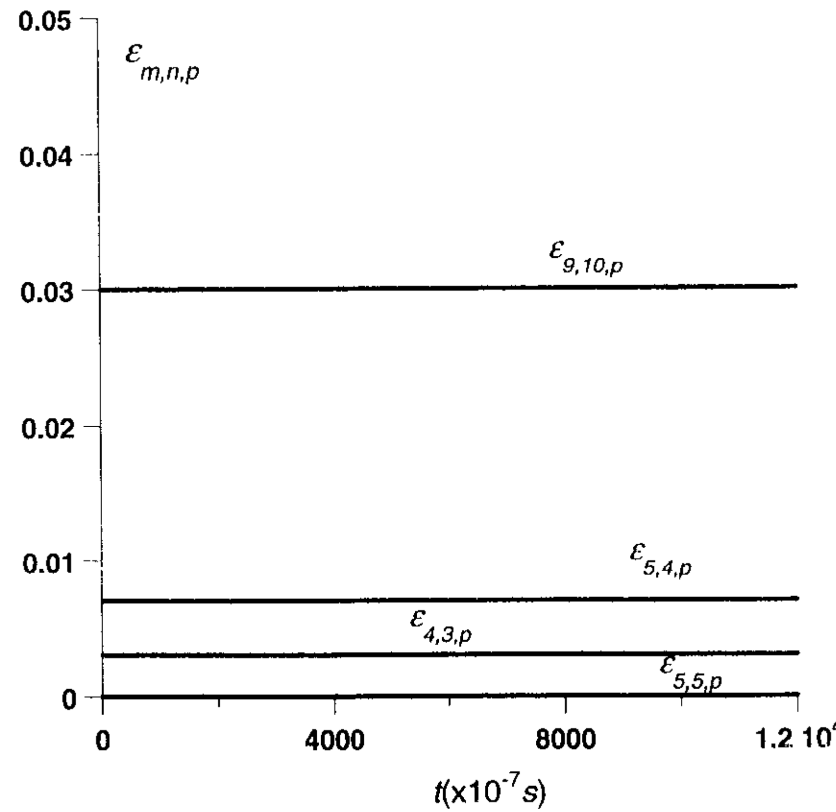
0.05
0.04
0.03
0.02
0.01
0
ε m,n,p
ε 9,10,p
ε 5,4,p
ε 4,3,p
ε 5,5,p
0
4000
8000
1.2 10^4
t(x10^-7 s)

Fig.2 a

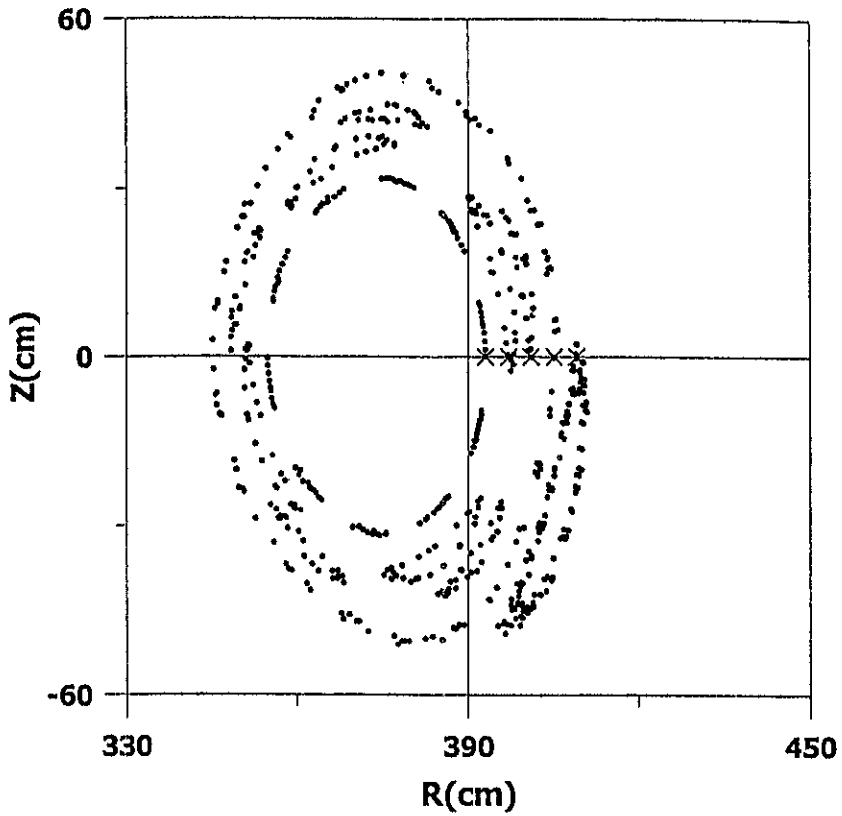
60
0
-60
Z(cm)
330
390
450
R(cm)

Fig.2 b

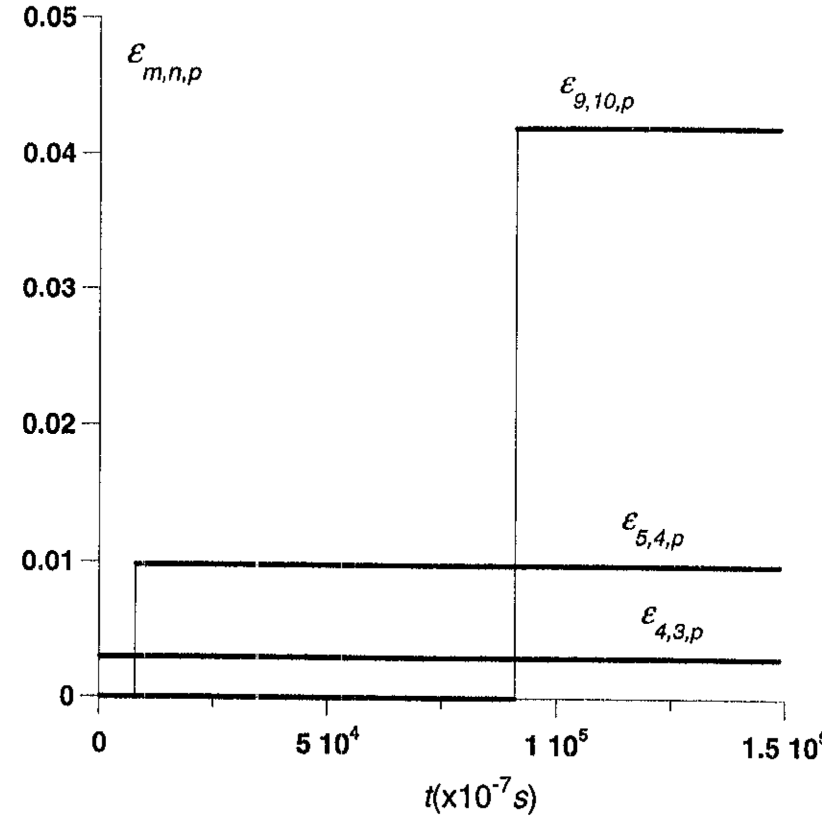
0.05
0.04
0.03
0.02
0.01
0
$\varepsilon_{m,n,p}$
$\varepsilon_{9,10,p}$
$\varepsilon_{5,4,p}$
$\varepsilon_{4,3,p}$
0
5 10^4
1 10^5
1.5 10^5
$t(x10^{-7}s)$

Fig.3 a

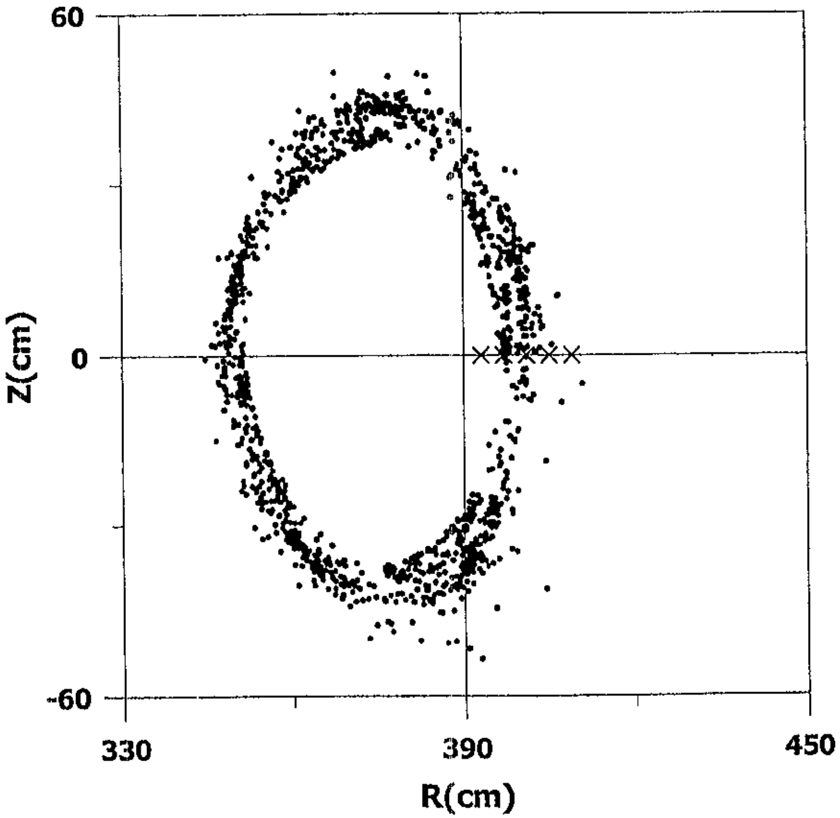
60
0
-60
Z(cm)
330
390
450
R(cm)

Fig.3 b

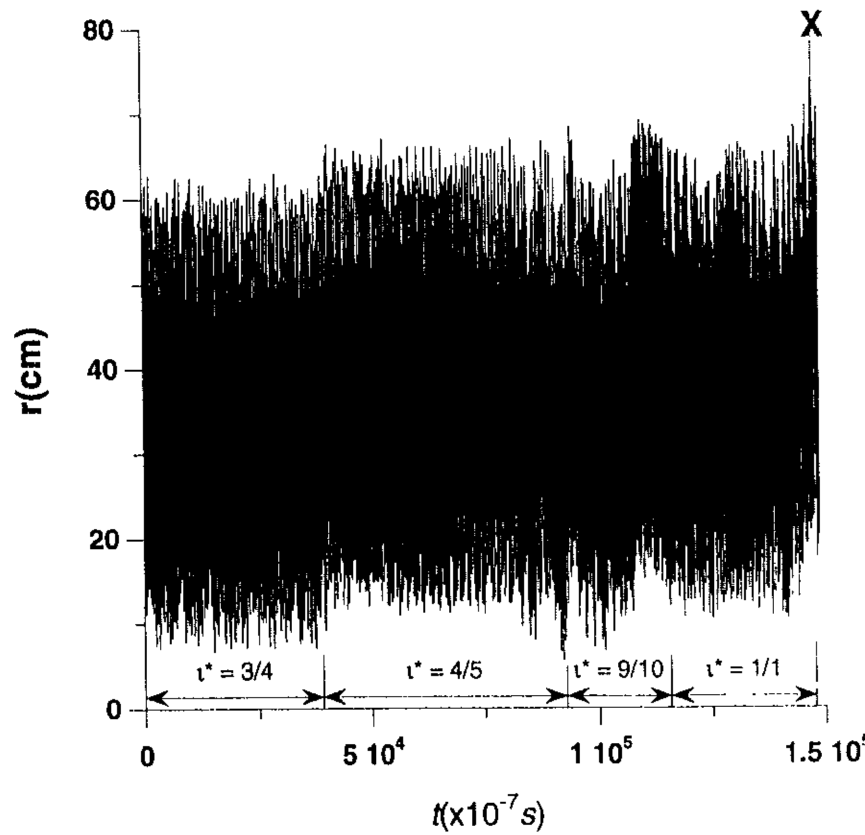
80
60
40
20
0
r(cm)
X
ι* = 3/4
ι* = 4/5
ι* = 9/10
ι* = 1/1
0
5 10^4
1 10^5
1.5 10^5
t(x10^-7 s)

Fig.3 c

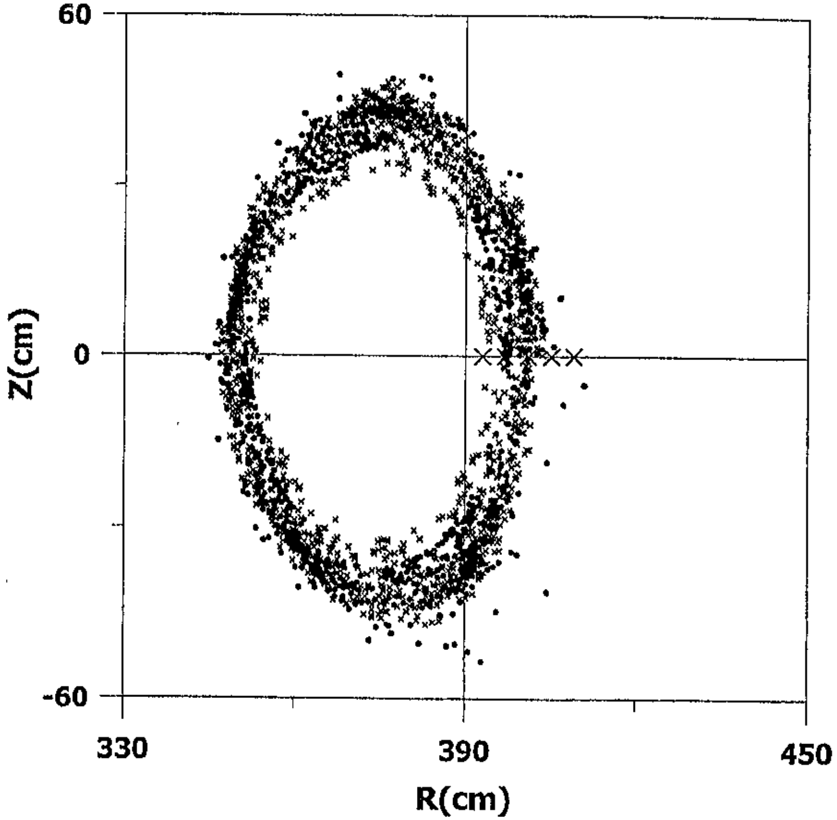

60
0
-60
Z(cm)
330
390
450
R(cm)

Fig.4 a

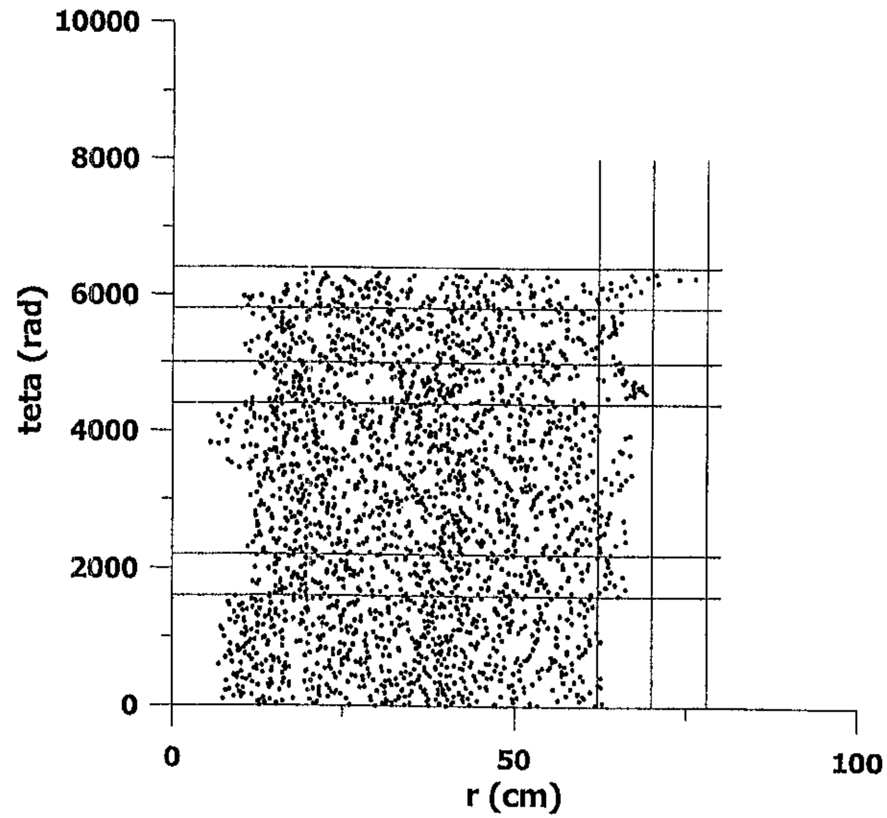

10000
8000
6000
4000
2000
0
teta (rad)
0
50
100
r (cm)

Fig.4 b

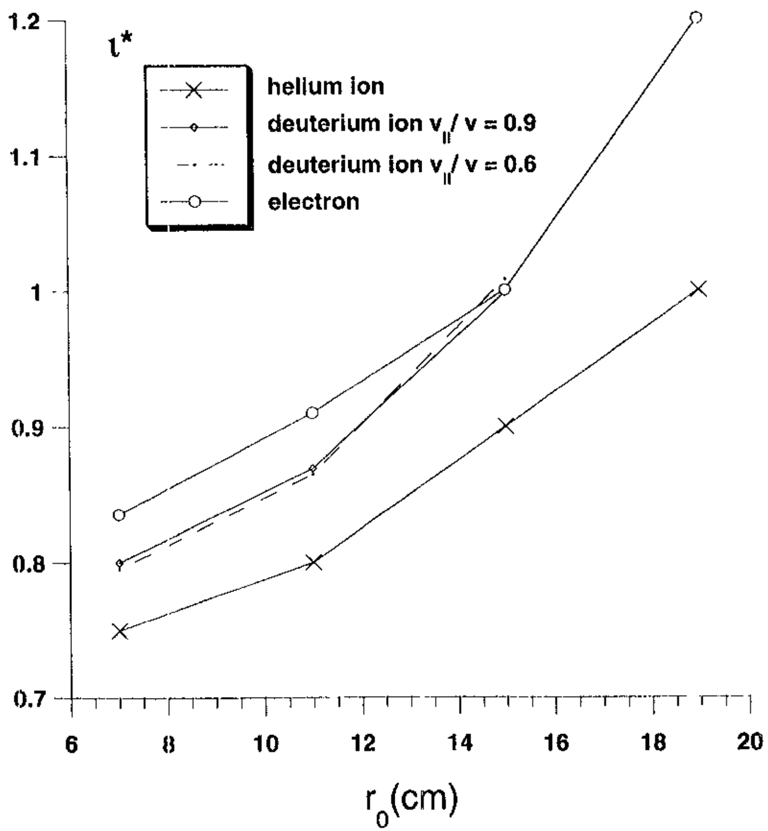
1.2
1.1
1
0.9
0.8
0.7
ι*
helium ion
deuterium ion v∥/ v = 0.9
deuterium ion v∥/ v = 0.6
electron
6
8
10
12
14
16
18
20
r0(cm)

Fig.5

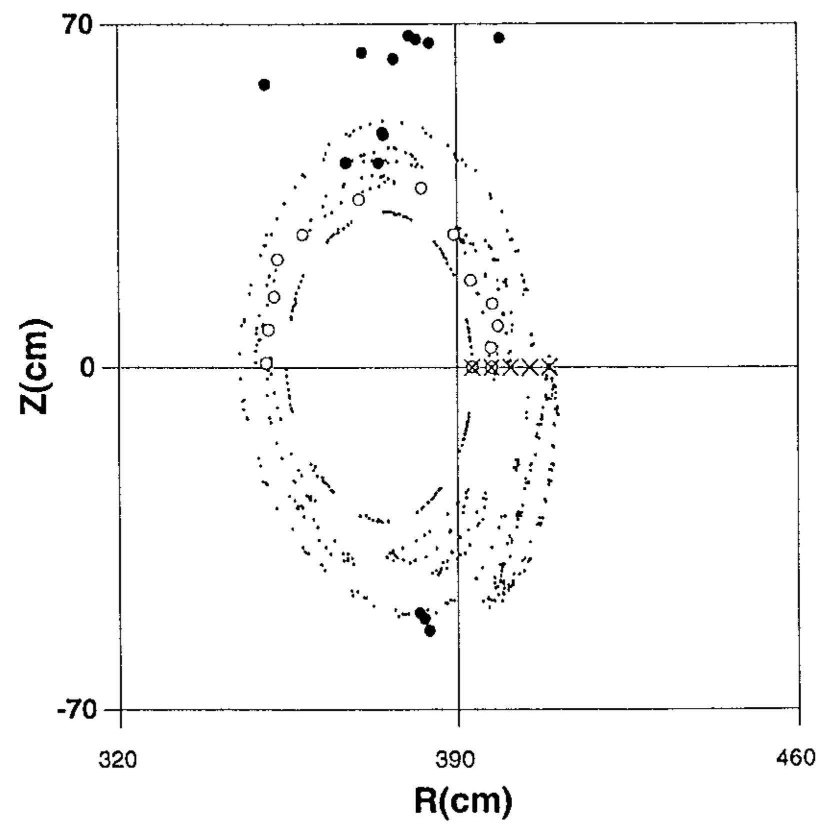
70
0
-70
Z(cm)
320
390
460
R(cm)

Fig. 6

Recent Issues of NIFS Series

NIFS-660 I Watari, I Mutoh R Kumazawa, T Seki, K Saito Y Torii, Y P Zhao, D Hartmann H Idei S Kubo, K Ohkubo M Sato T Shimozuma, Y Yoshimura, K Ikeda, O Kaneko, Y Oka, M Osakabe, Y Takeiri, K Tsumori, N Ashikawa, P C deVries, M Emoto, A Fukuyama, H Funaba, M Goto, K Ida, S Inagaki, N Inoue, M Isobe, K Itoh, S Kado, K Kawahata, T Kobuchi K Khlopenkov, A Komori, A Krasilnikov, Y Liang, S Masuzaki K Matsuoka, T Minami, J Miyazawa, T Morisaki, S Morita, S Murakami, S Muto, Y Nagayama, Y Nakamura, H Nakanishi, K Narihara, K Nishimura, N Noda, A T Notake, S Ohdachi, N Ohyabu H Okada, M Okamoto, T Ozaki, R O Pavlichenko, B J Peterson, A Sagara S Sakakibara, R Sakamoto, H Sasao, M Sasao K Sato, S Satoh, T Satow M Shoji, S Sudo, H Suzuki, M Takechi, N Tamura, S Tanahashi, K Tanaka, K Toi, T Tokuzawa, K Y Watanabe, T Watanabe, H Yamada, I Yamada, S Yamaguchi, S Yamamoto, K Yamazaki, M Yokoyama, Y Hamada, O Motojima, M Fujiwara,
The Performance of ICRF Heated Plasmas in LHD Sep 2000
(IAEA-CN-77/EX8/4)

NIFS-661 K Yamazaki, K Y Watanabe, A Sagara, H Yamada, S Sakakibara, K Narihara, K Tanaka, M Osakabe, K Nishimura, O Motojima, M Fujiwara, the LHD Group,
Helical Reactor Design Studies Based on New Confinement Scalings Sep 2000
(IAEA-CN-77/ FTP 2/12)

NIFS-662 T Hayashi, N Mizuguchi, H Miura and T Sato,
Dynamics of Relaxation Phenomena in Spherical Tokamak Sep 2000
(IAEA-CN-77THP2/13)

NIFS-663 H Nakamura and T Sato, H Kambe and K Sawada and T Saiki,
Design and Optimization of Tapered Structure of Near-field Fiber Probe Based on FDTD Simulation Oct 2000

NIFS-664 N Nakajima,
Three Dimensional Ideal MHD Stability Analysis in $L=2$ Heliotron Systems Oct 2000

NIFS-665 S Fujiwara and T Sato,
Structure Formation of a Single Polymer Chain I Growth of trans Domains Nov 2000

NIFS-666 S Kida,
Vortical Structure of Turbulence. Nov 2000

NIFS-667 H Nakamura, S Fujiwara and T Sato,
Rigidity of Orientationally Ordered Domains of Short Chain Molecules. Nov 2000

NIFS-668 T Mutoh, R Kumazawa, T Seki, K Saito, Y Torii, F Shimpo, G Nomura, T Watari, D A Hartmann, M Yokota, K Akaishi, N Ashikawa, P deVries, M. Emoto, H Funaba, M Goto, K. Ida, H Idei, K Ikeda, S Inagaki, N Inoue, M Isobe, O. Kaneko, K. Kawahata, A Komori, T Kobuchi, S Kubo, S. Masuzaki, T Morisaki, S Morita, J Miyazawa, S. Murakami, T Minami, S Muto, Y Nagayama, Y Nakamura, H. Nakanishi, K Narihara, N Noda, K Nishimura, K. Ohkubo, N. Ohyabu, S Ohdachi, Y Oka, M. Osakabe, T Ozaki, B.J Peterson, A Sagara, N. Sato, S Sakakibara, R. Sakamoto, H. Sasao, M. Sasao, M. Sato, T Shimozuma, M. Shoji, S Sudo, H Suzuki, Y. Takeiri, K. Tanaka, K. Toi, T Tokuzawa, K Tsumori, K Y. Watanabe. T Watanabe, H Yamada, I. Yamada, S. Yamaguchi, K. Yamazaki, M. Yokoyama, Y Yoshimura, Y Hamada, O Motojima, M Fujiwara,
Fast- and Slow-Wave Heating of Ion Cyclotron Range of Frequencies in the Large Helical Device Nov 2000

NIFS-669 K. Mima, M S Jovanovic, Y Sentoku, Z-M Sheng, M M Skoric and T Sato,
Stimulated Photon Cascade and Condensate in Relativistic Laser-plasma Interaction Nov 2000

NIFS-670 L Hadzievski, M.M Skoric and T Sato,
On Origin and Dynamics of the Discrete NLS Equation Nov 2000

NIFS-671 K. Ohkubo, S. Kubo, H Idei, T Shimozuma, Y. Yoshimura, F Leuterer, M Sato and Y Takita,
Analysis of Oversized Sliding Waveguide by Mode Matching and Multi-Mode Network Theory Dec. 2000

NIFS-672 C Das, S Kida and S. Goto,
Overall Self-Similar Decay of Two-Dimensional Tirbulence- Dec 2000

NIFS-673 L A Bureyeva, T Kato, V S Lisitsa and C Namba,
Quasiclassical Representation of Autoionization Decay Rates in Parabolic Coordinates Dec 2000

NIFS-674 L.A Bureyeva, V S Lisitsa and C Namba,
Radiative Cascade Due to Dielectronic Recombination Dec 2000

NIFS-675 M.F.Heyn, S V Kasilof, W Kernbichler, K Matsuoka, V V Nemov, S Okamura, O.S. Pavlichenko,
Configurational Effects on Low Collision Plasma Confinement in CHS Heliotron/Torsatron, Jan 2001

NIFS-676 K Itoh,
A Prospect at 11th International Toki Conference - Plasma physics, quo vadis?, Jan 2001

NIFS-677 S Satake, H. Sugama, M. Okamoto and M Wakatani,
Classification of Particle Orbits near the Magnetic Axis in a Tokamak by Using Constants of Motion, Jan 2001

NIFS-678 M Tanaka and A Yu Grosberg,
Giant Charge Inversion of a Macroion Due to Multivalent Counterions and Monovalent Coions Molecular Dynamics Studyn, Jan. 2001

NIFS-679 K Akaishi, M Nakasuga, H Suzuki, M Iima, N Suzuki, A Komori, O. Motojima and Vacuum Engineering Group,
Simulation by a Diffusion Model for the Variation of Hydrogen Pressure with Time between Hydrogen Discharge Shots in LHD, Feb. 2001

NIFS-680 A Yoshizawa, N Yokoi, S Nisizima, S.-I Itoh and K Itoh
Variational Approach to a Turbulent Swirling Pipe Flow with the Aid of Helicity, Feb 2001

NIFS-681 Alexander.A.Shishkin
Estafette of Drift Resonances, Stochasticity and Control of Particle Motion in a Toroidal Magnetic Trap, Feb 2001